Korean J. Chem. Eng., 39(12), 3190-3203 (2022)
DOI: 10.1007/s11814-022-1259-0

pISSN: 0256-1115
eISSN: 1975-7220

REVIEW PAPER

Dynamic simulation and control of a triple column process for dimethyl carbonate-methanol separation

Hong-Mei Wei*, Qiang Gao*, Wei-zhou Jiao,†, and Wei Wei***,†**

*Department of Mechanical Engineering, North University of China, No. 3 Xueyuan Road, Taiyuan, Shanxi, 030051,China
**Shanxi Province Key Laboratory of Higee-Oriented Chemical Engineering, North University of China, No. 3 Xueyuan Road, Taiyuan, Shanxi, 030051, China
***Low Carbon Energy Conversion Technology Research Center, Shanghai Advanced Research Institute, Chinese Academy of Science, Shanghai, 201203, P. R. China
(*Received 14 February 2022 • Revised 19 July 2022 • Accepted 10 August 2022*)

Abstract−Separation of dimethyl carbonate/methanol azeotropic mixture by using pressure-swing distillation process has been a hot-point in the study of the synthesis process of dimethyl carbonate by urea methanolysis method. This study updates the work of the writers (*Ind.Eng.Chem.Res,2013,52,11463-11478*), which explores the dynamic control structure of the three-column separation dimethyl carbonate (DMC)/methanol (MeOH) process from an actual pilot plant. At first, the conventional DMC/MeOH separation process in the pilot test of the DMC synthesis process through alcoholysis of urea was described in detail. Then an optimized control structure for the entire DMC/MeOH separation unit was obtained by implementing a general heuristic design procedure. An economic analysis was performed to evaluate the optimized process. Finally, three dynamic control schemes were proposed and evaluated with several large disturbances, an improved control scheme CS3, using the multiplier blocks "Q_{R1}/F_1" and "RR1" in T1, "Q_{R1}/F_1" and "R/F" in both T2 and T3, outperformed CS1 and CS2 by maintaining the product specification in each column.

Keywords: Dynamic Control, DMC/MeOH Separation, Steady-State Optimization, Triple-column Process

INTRODUCTION

Dimethyl carbonate (DMC) and its synthetic route have drawn much attention in recent years in the field of chemical synthesis [1,2]. As an environmentally benign building block, DMC can be an alternative to acylating and methylating agents due to its non-toxicity and biodegradability [3-6]. DMC can also substitute MTBE to be an oxygenated fuel additive for gasoline or diesel be an oxygenated fuel additive for petrol or diesel due to its low oxygen content. A green route for the synthesis of DMC by catalytic alcoholysis of urea was considered to be an attractive route for many advantages [7]: readily available raw materials-Urea and MeOH, higher reaction activity, higher selectivity, and the byproduct ammonia is zero byproduct emission. In addition, the other main by-products CO_2 and MeOH decomposed by DMC have no serious environmental impacts, as compared to other fuel additives. Overall, this route is environmentally friendly.

Notably, due to the presence of the DMC/MeOH azeotrope in the reaction system, it is inefficient to recycle DMC by conventional distillation techniques. DMC/MeOH azeotrope separation has become a hot topic in DMC synthesis through alcoholysis of urea.

Recently, several schemes have been presented for DMC/MeOH azeotrope separation via pressure swing distillation (PSD), which includes pressured-atmospheric and atmospheric-pressured series separation process. The pressured-atmospheric series separation process was presented by Li et al. [8] and Wang et al. [9].

In their works, the UNIQUAC and NRTL interaction parameters were regressed based on experimental data, respectively; steady-state simulation was carried out to obtain the best process conditions.

According to the process characteristics of DMC synthesis through alcoholysis of urea, an atmospheric-pressured series separation process was presented by Zhang et al. [10] and the DMC/MeOH azeotrope separation process with DMC at low concentrations was rigorously simulated and optimized using the Wilson model. After a literature review about DMC/MeOH azeotrope separation via PSD, it was found that the previous investigations mainly focused on steady-state performance. To this date, only a few focused on control and dynamic characteristics, which includes the work of Hsu et al. and the writer. In Hsu et al's [11] work, the DMC/MeOH azeotrope via transesterification of MeOH with ethylene carbonate, was separated by extractive distillation. In our previous work [12], a rigorous simulation was implemented based on the Wilson equations, two suitable control schemes of the pressured-atmospheric process were presented. Summarizing the above literatures, these studies mainly focused on the concept design, optimization, and control. Additionally, most systems were binary homogeneous azeotropes, and the DMC/MeOH separation took place in one single column or two distillation columns. Very few studies focused on the actual multi-unit separation dimethyl carbonate (DMC)/methanol (MeOH) process on the scale of an actual pilot plant. So, further research is needed on the dynamic characteristics and more complex column configurations.

†To whom correspondence should be addressed.
E-mail: jwz0306@126.com, weiwei@sari.ac.cn

This paper investigated the control of a three-column separation process. According to conventional process control wisdom, the multi-column operation in the pilot plant research is a far more complex system and exhibits severe interference, specifically multi-parameter and heavy coupling. As such, this present study explores the dynamic characteristics of the actual device, and then an effective dynamic control scheme of the three-column separation process in the actual pilot test will be explored.

PROCESS FLOWSHEET

The initial data is collected from a pilot plant of 300 tons/year DMC synthesis process via urea [13-15]. The fresh feed is injected at the flow rate of 378 kg/h, the majority of the mixed stream composed of 89.1 wt% MeOH, 10.9 wt% DMC, but small traces of NH_3 (0.099 wt%) and CO_2. The nonideal mixture of DMC and MeOH creates a minimum-boiling homogeneous azeotrope under room temperature and ambient pressure. The Wilson physical property package is used in the Aspen Plus simulation, and the calculated phase diagrams at 0.1 and 1.5 MPa are shown in Fig. 1; the higher the pressure, the lower will be the DMC content in the azeotrope, which indicates that the DMC/MeOH azeotrope can be separated by pressure-swing distillation.

The conventional DMC/MeOH separation sequence shown in Fig. 2 consists of three distillation columns performing several tasks: pre-concentration of DMC (T1), pressured distillation (T2), refined distillation (T3). The feed stream is a mixture of the fresh feed and a recycled stream from T2 distillation, which was fed at 18 of a 25-stage DMC concentration column operating at a condenser pressure of 0.11 MPa and an operating temperature of 338 K. The DMC concentration column plays the role of increasing the DMC concentration in the mixture (under atmospheric pressure) higher than its azeotropic point at 1.2 MPa. As a light component, DMC/MeOH azeotrope comes out from the top of T1 with the DMC content as

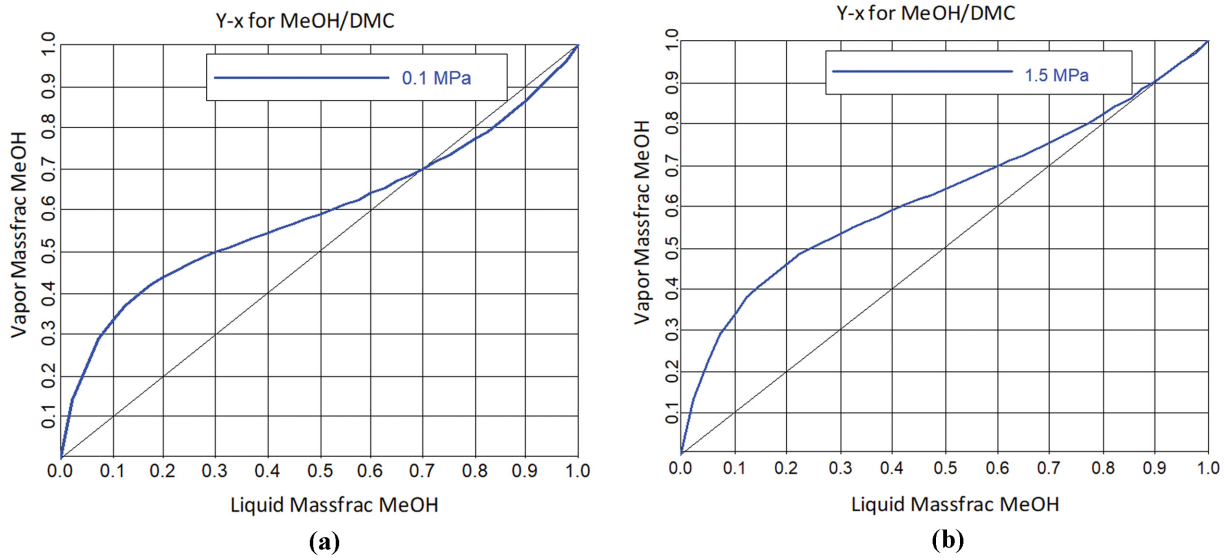

Fig. 1. (a) DMC/MeOH at 0.1 MPa; (b) DMC/MeOH at 1.5 MPa.

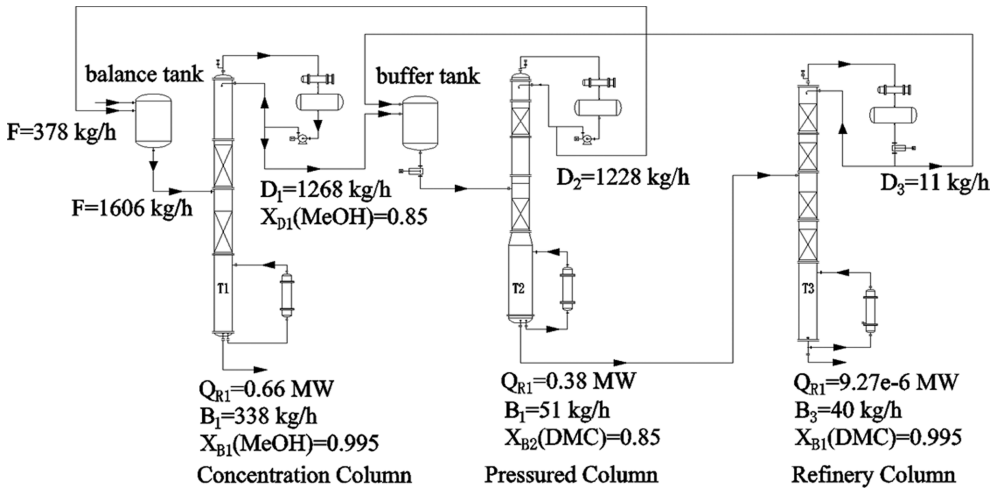

Fig. 2. Flowsheet of the three-column separation DMC/MeOH process.

Table 1. Basis of economics

Condensers
heat-transfer coefficient=0.852 kW/K·m^2
differential temperature=87.3 °C (atmospheric column)/112 °C (pressurize distillation column)
capital cost=7296 $A_C^{0.65}$ where Area is in m^2
Reboilers
heat-transfer coefficient=0.568 kW/K·m^2
differential temperature=57.7 °C (pressurize distillation column)/36.5 °C (atmospheric column)
capital cost=7296 $A_R^{0.65}$ where Area is in m^2
Column vessel
capital cost=17,640 $D^{1.066}$ $L^{0.802}$ where D and L are in m
energy cost=\$4.7/10^6 KJ
payback period=3 years

where the A_R and A_C are the areas of the heater exchanger and the condenser, respectively, with units of m^2; D is the inside diameter of the column, with units of meter; L is the length of the vessel, with units of meter.

high as 30%, which will be further distilled in the pressured column to produce higher concentration of DMC. The first reboiler transfers 0.67 MW of hot. The DMC/MeOH azeotrope is then further separated by means of a pressure swing distillation process, that is, it is first separated in the pressured distillation (at 1.2 MPa) and then in the refined distillation (at 0.2 MPa).

The distillate of T1 (1,627 kg/h) mixed with the distillate of T3 (153 kg/h) was fed through the 15th stage of T2 (1,780 kg/h). The pressured column T2 operated at 1.2 MPa and 428 K, its reboiler duty was 1.09 MW. The DMC/MeOH azeotrope (approximately 5 wt% DMC) came out as distillate of T2, which (1,588 kg/h) was recycled back to T1, and the DMC/MeOH azeotrope (approximately 85 wt% DMC) was produced as bottom product, which was then fed at stage 14 of T3 for further distillation.

The refined column (T3) operated at 0.2 MPa, its reboiler duty was 0.04 MW, rendering bottom and top temperatures of 388 K and 356 K, respectively. The DMC/MeOH azeotrope (approximately 30 wt% DMC) was distilled as top product, which was then recycled back to T2 after cooling, nearly pure DMC (99 wt%) came out as bottom product.

STEADY-STATE OPTIMIZATION

A shortcut design was first used to obtain process parameters; the steady-state process was simulated by Aspen plus; the parameters of Wilson thermodynamic model were taken from Ma et al. [16]; other physical properties were from the Aspen Plus databank: vapor pressure, vapor and liquid enthalpies and densities; all the gases in this system were considered ideal gases. The desired product purity was that the bottoms purity of T1 was 99.5 wt% MeOH, the distillate purity of T2 was 85 wt% MeOH, and the bottoms purity of T3 was 99.5 wt% DMC.

The many design parameters in each distillation column were adjusted to reach these specifications discussed above while optimizing the economic objective function-total annual cost (TAC): the number of trays, the position of the feeding plates, reflux ratio and reboiler heat input. The TAC reflects both energy and capital costs, which is calculated using the following equation [17]:

$$\mathrm{TAC}=\frac{\text{captical cost}}{\text{payback year}}+\text{energy cost}$$

where the capital cost includes the capital cost of the heat exchanger. And the column vessel, and the energy cost is the heat cost added to the reboiler. Both equations for estimating capital cost and energy cost were covered by Douglas [18], Turton [19] and Luyben.

Table 1 gives the economic parameter values and the sizing relationships and parameters used.

The sizes of the two columns were determined by using the tray sizing function in Aspen Plus and a sieve plate was selected. The heat transfer areas for the condenser and reboiler are determined based on the overall heat transfer coefficient and the differential temperature. The heat exchange areas of condenser and reboiler are calculated according to the following formula:

$$A_R=\frac{Q_R\times 1.055\times 2.54e^6}{3{,}600\times 0.7457\times \Delta T_R\times U_R} \tag{3}$$

$$A_C=\frac{Q_C\times 1.055\times 2.54e^6}{36{,}000\times 0.7457\times \Delta T_C\times U_C} \tag{4}$$

where the Q_R, Q_C are the reboiler duty and condenser duty with units of GJ/hr; ΔT_R, ΔT_C are the differential temperatures for the reboiler and condenser with units of °C; U_R, U_C are the overall heat transfer coefficients for reboiler and condenser with units of KW/(°C·m^2) [17].

A recycle stream flowed back to the first and second columns. As such, the three-column system was first designed by performing rigorous process simulation with the first and third bottom product kept at their specification. The design variables that required determination included the total stages (N_{T1}, N_{T2}, and N_{T3}) and the feed location (N_{F1}, N_{F2}, and N_{F3}). The design parameters distillate rate (D) and reflux ratio (RR) in each column were manipulated to achieve the desired product specifications while being optimized in terms of their TACs. The optimal design and operating conditions were obtained by using a sequential iterative optimization procedure: the total stages N_T was used as the outer iterative loop, and

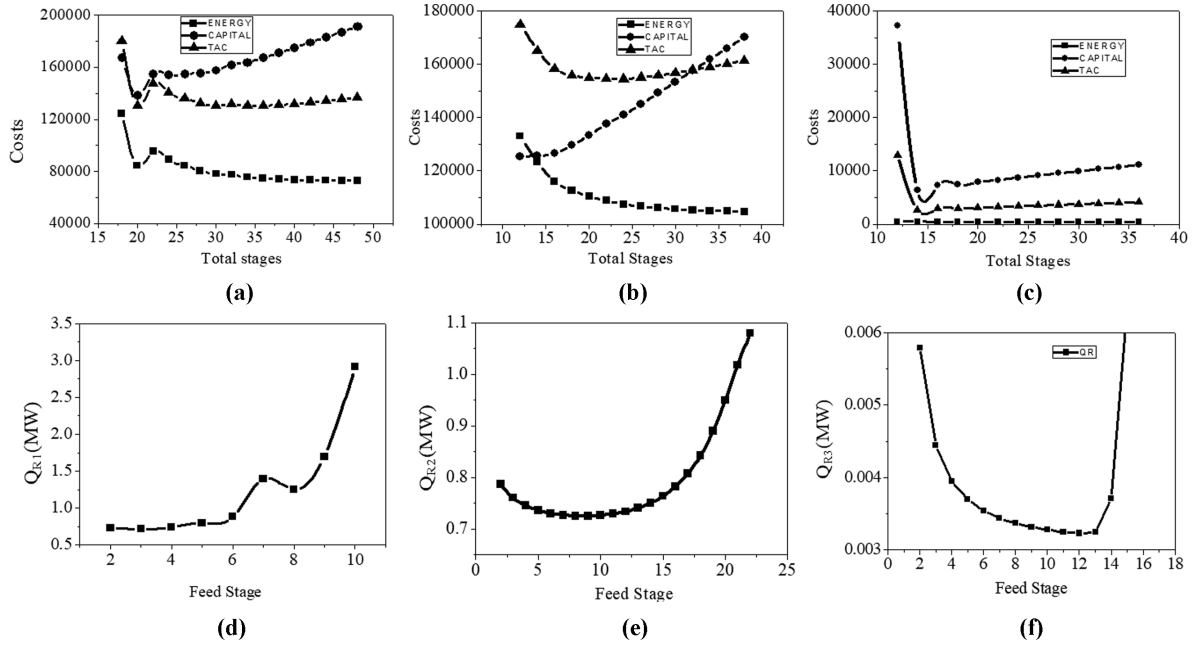

Fig. 3. Effect of stages and feed location on TAC. (a) TAC_1 vs. N_{T1}; (b) TAC_2 vs. N_{T2}; (c) TAC_3 vs. N_{T3}; (d) Q_{R1} vs. N_{F1}; (e) Q_{R2} vs. N_{F2}; and (f) Q_{R3} vs. N_{F3}.

Table 2. Design variables and TAC

(a) Original Process			
	T1	T2	T3
N_{stage}	25	22	18
Feed stage	5	12	12
D (m)	0.506	0.503	0.046
Q_R (MW)	0.657	0.873	0.003
Q_C (MW)	−0.005	−0.793	−0.005
A_C (m^2)	20.249	16.106	0.065
A_R (m^2)	9.61	13.706	0.155
Shell (10^6 $)	8.21e+4	7.29e+4	4.78e+3
HX (10^6 $)	8.33e+4	8.44e+4	3.41e+3
Energy (10^6 $/y)	9.74e+4	1.29e+5	4.78e-3
Capital (10^6 $)	1.65e+5	1.57e+5	8.19e+3
TAC (10^6 $/y)	1.53e+5	1.82e+5	3.21e+3
Total TAC (10^6 $/y):	3.38e+5		
(b) Optimized Process			
	T1	T2	T3
Nstage	34	24	16
Feed stage	4	8	12
D (m)	0.451	0.421	0.045
Q_R (MW)	0.523	0.706	0.003
Q_C (MW)	−0.511	−0.641	−0.005
A_C (m^2)	15.672	13.367	0.068
A_R (m^2)	7.462	11.380	0.162
Shell (10^6 $)	9.333e+4	6.613e+4	201.257
HX (10^6 $)	7.059e+4	7.480e+4	3.501e+3
Energy (10^6 $/y)	0.756e+5	1.075e+5	4.992e-3
Capital (10^6 $)	1.639e+5	1.409e+5	3.703e+3
TAC (10^6 $/y)	1.303e+5	1.545e+5	1.733e+3
Total TAC (10^6 $/y):	2.86e+5		

N_β inner iterative loop. In the rigorous steady-state simulation, the two manipulated variables total stages N_T and feed stage N_F were varied simultaneously, wherein the optimum total number of trays and the optimum feed tray location of each unit were determined to minimize TAC.

The results of the optimization run for the three columns are presented in Fig. 3, wherein each minimum TAC was obtained by varying the feed location when the total number of stages was fixed. The optimum stage number and optimum feed stage of the three columns were as follows: 34 and 4th for T1, 24 and 8th For T2, 16 and 12th for T3. The tray number was counted from top to down with the condenser as the 1st tray and the reboiler as the last tray. All three distillation columns studied in this work used the total condensers, and their liquid temperature was at boiling point.

A detailed comparison of the original design and the optimal design is shown in Table 2. However, the total stage number of T2 and T3 via the optimized design was both more than the original one. As such, both T2 and T3 exhibited that the optimal design energy and operating cost savings was 19.08% and 6.6%, respectively, and the total TAC savings could reach 15.28%. These results indicate the superiority of the optimal design as compared to the original one.

CONTROL SYSTEM DESIGN

Maintaining the DMC purity is the overall control objective for this flowsheet. Each unit in the flowsheet has its own task and must be controlled to achieve these tasks. Therefore, an effective way of controlling each column to achieve its objective (the bottoms product of T1 is 99.5 wt% MeOH, the distillate product of T2 is 85 wt% MeOH, and the bottoms product of T3 was 99.5 wt% DMC) and then maintain all the units stable operation.

1. Temperatures Profiles

According to conventional wisdom, a single-end temperature controller with a "reflux-to-feed ratio" or a "reflux ratio" structure can better handle disturbances in feed flowrate and feed composition [17]. The temperature control tray points are commonly obtained following the slope criterion, that is, the suitable temperature control points are chosen as the location where the temperature profile is steep [17]. Which was borrowed from Luyben's theory in the selection of effective control structures: "Large changes in temperature from tray to tray indicate a region where compositions of important components are changing. Maintaining a tray temperature at this location should hold the composition profile in the column and prevent light components from dropping out the bottom and heavy components from escaping out the top?" The single-end temperature control scheme and the slope criterion were employed in this study.

Fig. 4 illustrates the temperature profiles of the three columns. It is clear that the tray with the sharpest temperature change in column T2 was stage 20 (419 K), in column T3 was stage 15 (369 K), which could be selected as the appropriate sensitive plate for T2 and T3, respectively. However, there was not a sharp break in the temperature profile of T1, and the temperature profile was almost a straight line, such that the slope criterion was no longer valid for selecting the sensitive plate. In addition, other sensitivity criteria were required to determine the most sensitive plate. For the sensitive plate of the concentration column, the constant temperature criterion was selected as follows [17]. By keeping the distillate and bottoms concentration as the feed composition is changed within an expected range, the plate that does not change with the feed concentration is the sensitive plate.

A series of sensitivity analysis were performed to study the influence of the feed composition on the product purity that was reached in T1. The "Design spec/Vary" feature of Aspen Plus was used to maintain the product concentration at 99.5 wt% MeOH by changing 50% feed compositions of DMC. As the feed composition changed, where the tray temperature did not change much with the feed composition were the right locations for temperature control. Fig. 5 shows the effect of the feed compositions changes on the tray temperature, wherein the 21st tray temperature remained constant. Therefore, stage 21 was selected as the sensitive plate of T1.

2. Basic Control Structure - CS1

Before performing a dynamic simulation, equipment sizing was necessary. The column diameters were needed to be determined in Aspen Plus using the tray sizing functions, the column bases and reflux drum were sized with conditions that their volume be large enough to provide 5 min of holdup when half full, and the decanter was specified to provide 10 min of holdup. Control valves and pumps were sized to give the rangeability required to handle the large disturbance tested in the dynamic simulations. The pressure drops of most valves were specified to be 2 bar. The flowsheet was exported into Aspen Dynamics after being pressure checked.

2-1. Structural Description of CS1

A reflux-to-feed ratio controller was first applied in each column, wherein the bottom level of T1 became zero after a step disturbance was implemented. Then the system ran with stability when

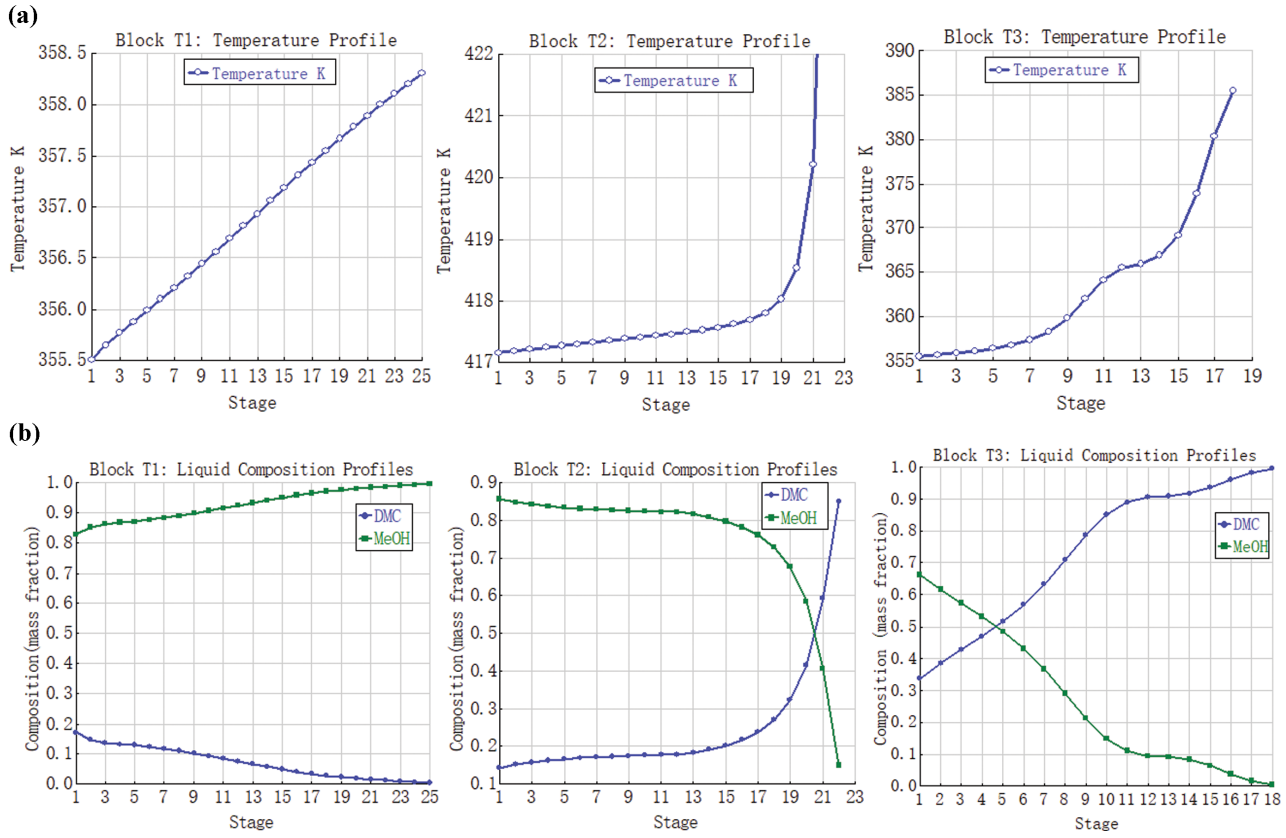

Fig. 4. (a) Temperature profiles; (b) composition profiles.

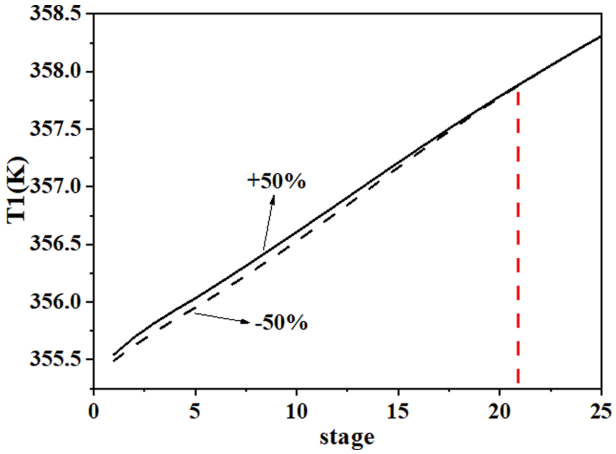

Fig. 5. Temperature profiles of T1 for feed composition disturbances.

a reflux ratio fixed controller was used instead in each column. Fig. 6 shows this effective control scheme followed by Luyben [21,22] and Grassi [23]. These trays were selected as sensitive plates: stage 21 in column T1, stage 20 in column T2, and stage 15 in column T3. The various control loops were implemented as follows:

Column T1:

1. Feed is flow controlled.
2. Pressure is controlled by condenser heat removal.
3. Reflux-drum level is controlled by manipulating distillate.
4. Base level is controlled by manipulating bottoms.
5. Reflux ratio is held constant.
6. The temperature of the stream of T1-D is controlled at 356 K by manipulating the heat removal in the cooler (T1DHT).
7. Stage 21 temperature is controlled at 358 K by reboiler heat input (KC=17 and τ_I=7.92 min).

Column T2:

1. The feed out of the mixer is flow controlled.
2. Pressure is controlled by condenser heat removal.
3. Reflux ratio is kept constant.
4. Reflux-drum level is controlled by manipulating distillate.
5. Base level is controlled by manipulating bottoms.
6. The temperature of the stream of T2-D is controlled at 417 K by manipulating the heat removal in the cooler (T2DHT).
7. The temperature on 20th tray is controlled at 420 K by reboiler heat input (K_C=11.81 and τ_I=6.6 min).

Column T3:

1. The temperature on 15th tray is controlled at 369 K by reboiler heat input (K_C=16.43 and τ_I=19.79 min).
2. The temperature of the stream of T3DL is controlled at 355 K by manipulating the heat removal in the cooler (T3DHT).
3. Pressure is controlled by condenser heat removal.
4. Reflux ratio is kept constant.
5. Reflux-drum level is controlled by manipulating distillate.
6. Base level is controlled by manipulating bottoms.

The standard control strategy was employed in most of the loops discussed above, conventional flow controller tuning (K_C=0.5 and τ_I=0.3 min) was used in all flow controllers; all level controllers were proportional with gains of 2; column pressure controllers were PI and used Aspen Dynamic default controller settings; deadtime element of 1 min was used in all temperature loop; and the temperature controller settings (ultimate gain and period) were achieved using the relay-feedback test. All controller tuning constants were given using Relay-feedback testing and Tyreus-Luyben settings [22]. The temperature loop in each column was tuned using an iterative tuning procedure. The procedure was repeated until the tuning parameters from the relay feedback test converged. Temperature transmitters ranged between 200 K and 500 K for column T1 and T3, 200 K and 600 K for T2.

2-2. Dynamic Performance of CS1

The dynamic controllability of the basic control scheme was evaluated by the disturbance resistance in terms of changes in feed flow rate and feed composition. These results are presented in Fig. 7, wherein the solid lines represent the 20% step increase case, and

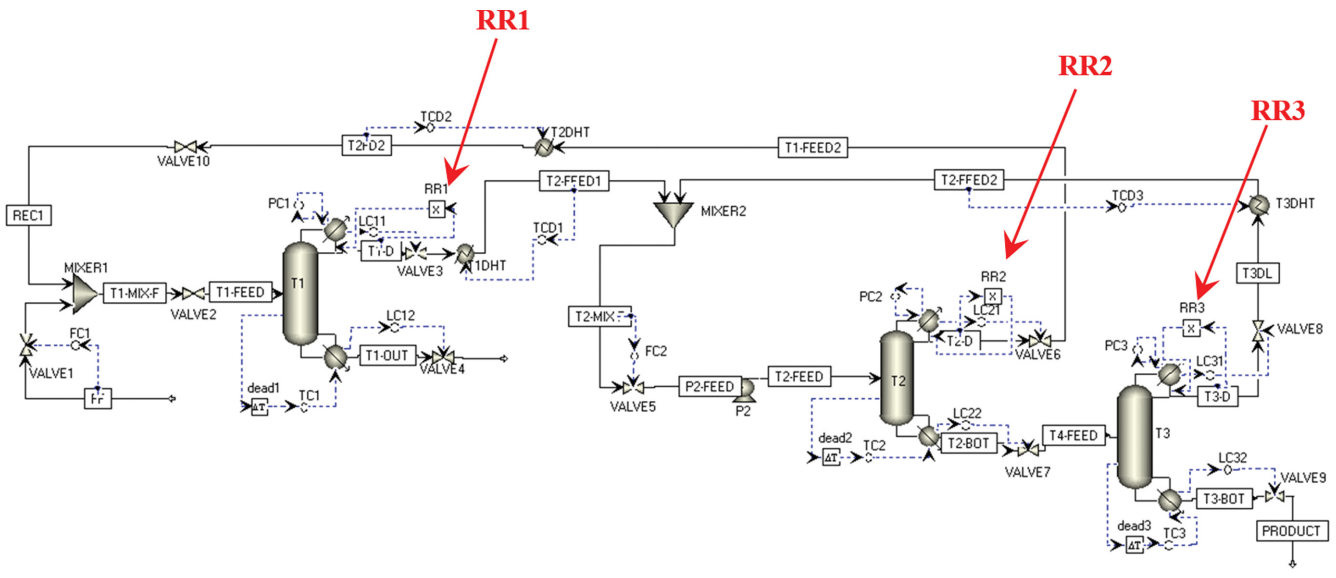

Fig. 6. Basic control structure - CS1.

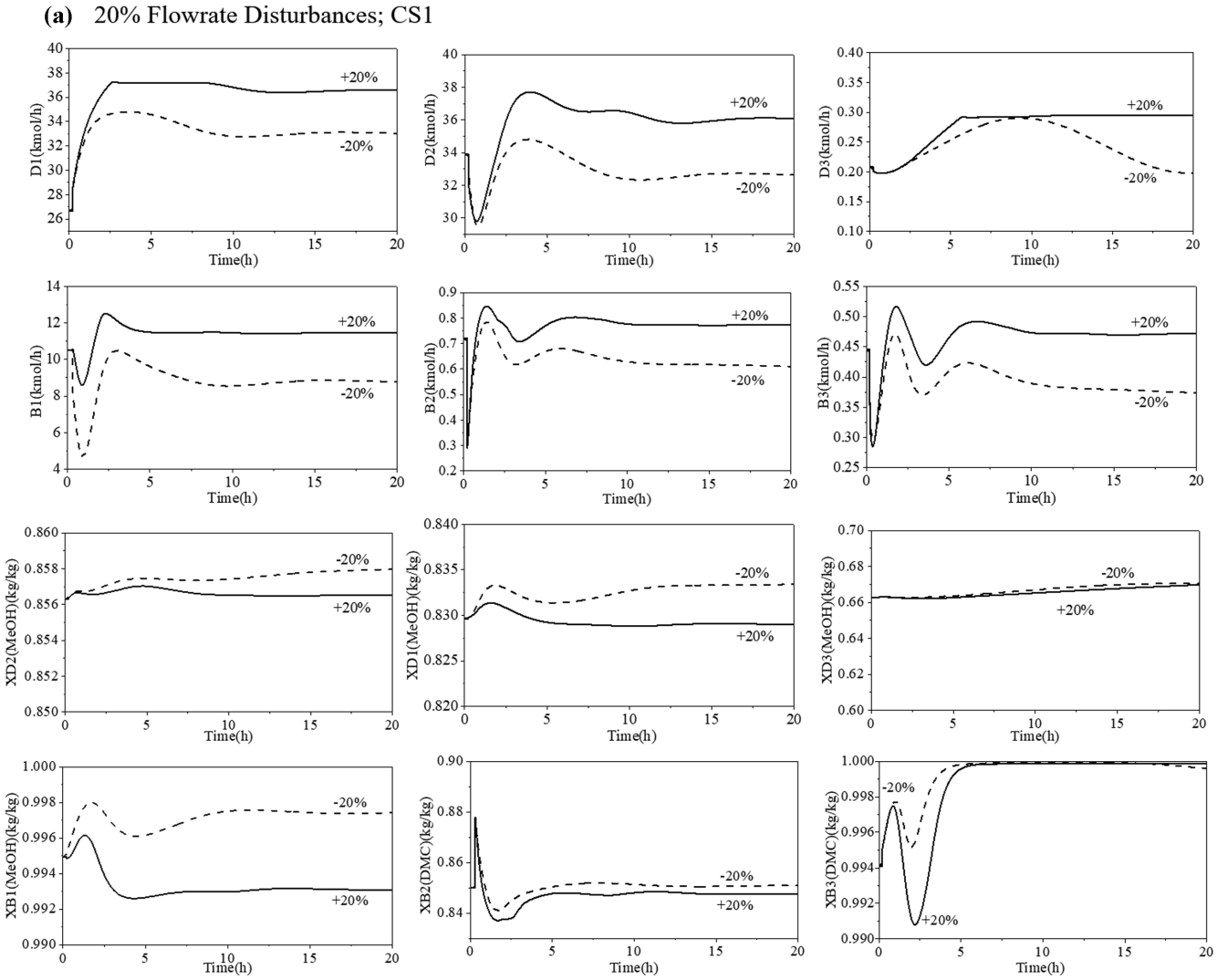

Fig. 7. CS1: (a) 20% Feed rate disturbances. (b) 20% feed composition disturbances.

the dashed lines, decrease. Fig. 7(a) reveals the dynamics of the ±20% feed flow rate change. That is, the value of the total feed flow controller setpoint was changed from 11.497 kmol/h to 13.796 kmol/h and decreased to 9.198 kmol/h, respectively.

Notice that the distillate product, D, bottom product, B, and the bottom purity, X_B, of the three columns significantly fluctuated with the feed flow disturbances, while the change trend of the distillate purity on top of the three columns was relatively slow. In particular, the bottom product B suddenly decreased, fluctuated, and finally stabilized after it ran for 10 h. It was noticed that the system rides through these disturbances fairly well except for the bottom purity X_{B1} (MeOH) of T1, and which dropped to almost 99.2 wt% after a 20% increase in the feed flowrate, while X_{B3} (DMC) tended to 1 regardless of the 20% increase and decrease in the disturbances of the feed flowrate.

Similar results were obtained when step increase and decrease happened in the feed concentration. The solid lines in Fig. 7(b) define a 20% step changes in feed DMC concentration from 0.109 wt% to 0.131 wt%, and the dashed lines, from 0.109 wt% to 0.087 wt%. It is observed that X_{B1} (MeOH) dropped to 99.3 wt% when a +20% increase was implemented in the feed composition. X_{B3} (DMC) tended to 1 regardless of the 20% increase and decrease in feed DMC concentration.

As can seen in Fig. 7, the basic control structure CS1 can maintain the product concentration X_{B2} (DMC) and X_{B3} (DMC) very well regardless of feed flow rate and feed composition disturbances, while the product concentration X_{B1} (MeOH) cannot kept quite close to its specification. Consequently, the basic control structure CS1 needs to be further improved before it can solve the problem of maintaining bottoms purity X_{B1} (MeOH). In the next section, several alternative ways will be discussed.

3. Modified Control Structure CS2

3-1. Structure Description of CS2

A feedforward ratio controller, Q_R/F, was introduced in the modified structure CS2 to improve the dynamic performance, which was proposed by Luyben [25]. Using the revised control structure, the reboiler heat duty Q_R will vary immediately in accordance with the feed flowrate. As previously discussed, one tray temperature

(b) 20% Feed Composition Disturbances; CS1

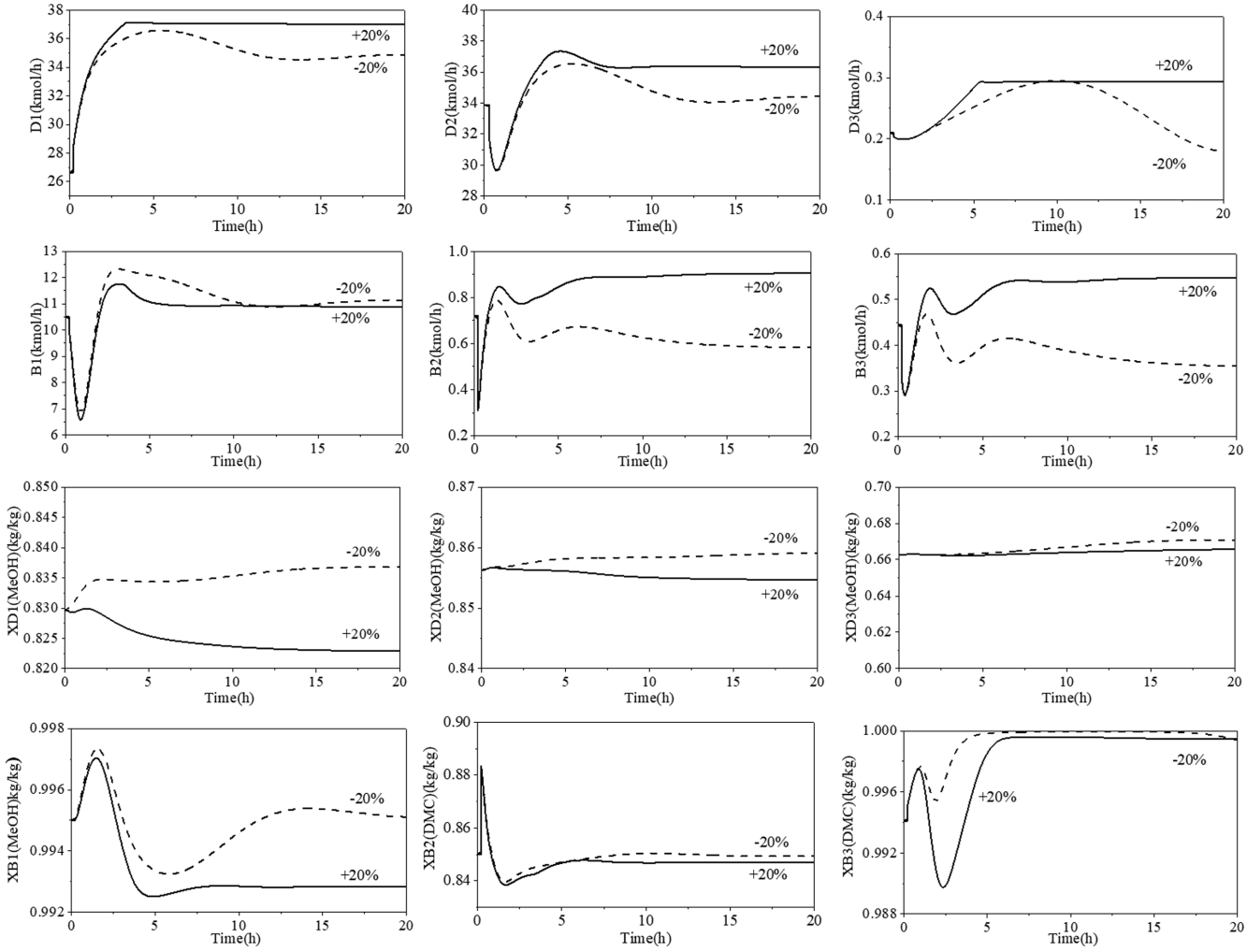

Fig. 7. Continued.

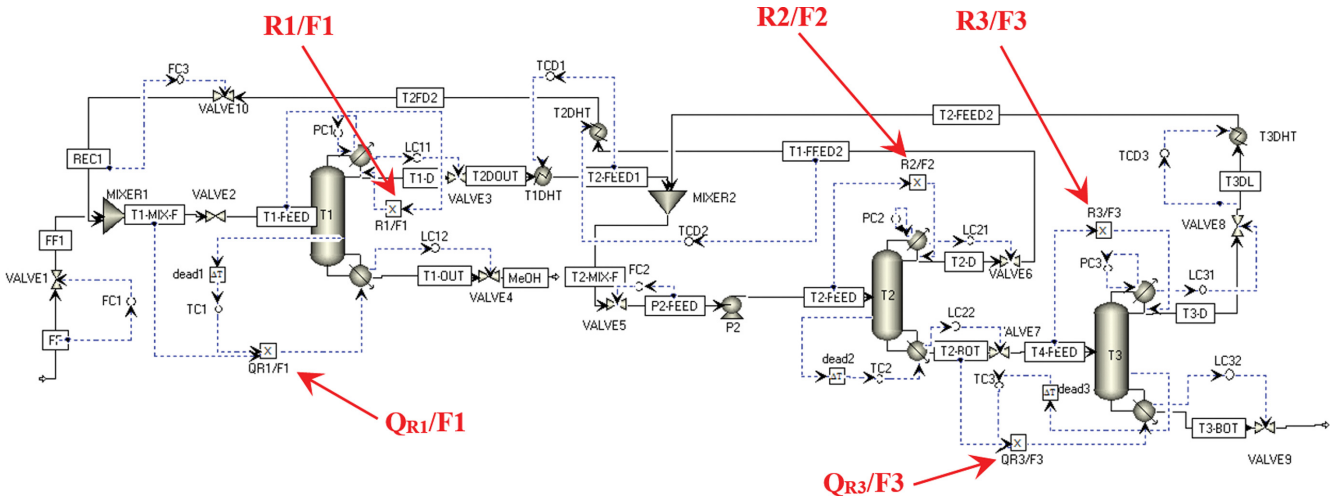

Fig. 8. Control structure-CS2.

control loop with the reflux ratio RR fixed or the reflux to feed ratio R/F maintained, which should maintain the distillation column stably. Moreover, the R/F ratio scheme generally has better dynamic performance than the RR scheme [17]. Consequently,

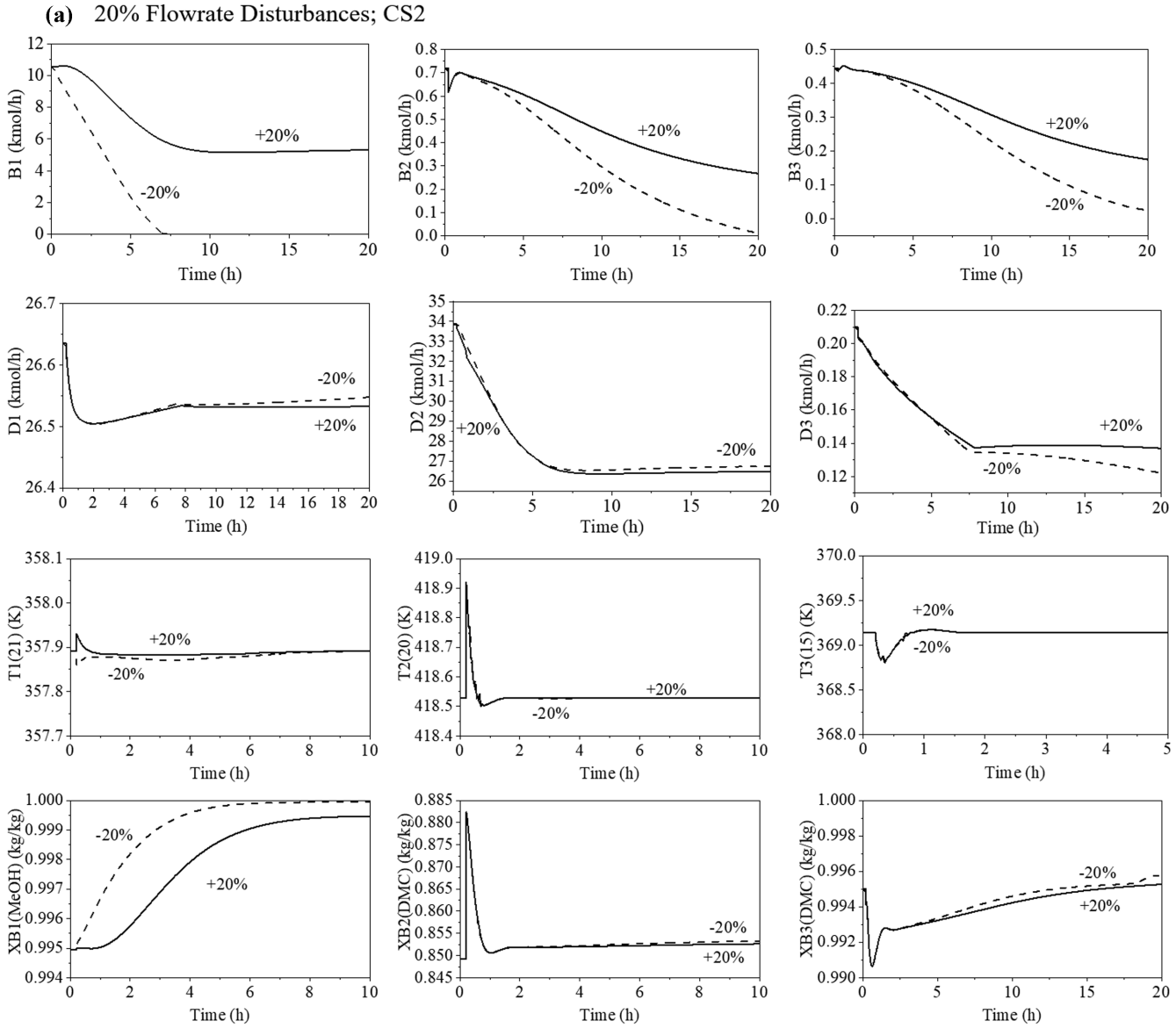

Fig. 9. (a) CS2: 20% feed flowrate disturbances. (b) 20% feed composition disturbances.

the R/F ratio structure was also implemented in the modified control structure CS2.

Fig. 8 presents the modified control structure CS2. The two loops TC1-Q_{R1}/F1 and TC3-Q_{R3}/F3 were used in T1 and T3, respectively. In each loop, their one input is the output signal of the multiplier, Q_R/F, and the other input is the feed to column T1 and T3, respectively. The R/F multiplier was implemented in each column. The temperature controllers TC1 and TC3 were retuned by running the relay-feedback test.

3-2. Dynamic Performance of CS2

The dynamic performance of a 20% step change in the flow controller (FC1) setpoint at 0.2 h is illustrated in Fig. 9(a). The dynamic performance of a 20% step change in the feed composition is presented in Fig. 9(b). The dashed lines define the 20% decrease. As shown in Fig. 9, a decrease in the fresh feed resulted in a decrease in the three bottom products B1, B2, and B3. In particular, the bottom product B1 fell to zero at t=7 h, and the bottom products B2 and B3 fell to a very low value after running for a while.

The variation trend above is the same as the control scheme CS2, where the reflux-to-feed controllers were used in each column. Furthermore, many other schemes have been attempted to improve the performance of CS2. However, the implementation of either the fixed reflux ratio or the fixed reflux-to-feed ratio in T2 exhibited the same problem, where the bottom level of T1 fell to zero after run initiation.

This problem may be a result of rapid steam rising from the bottom due to the use of the Q_R/F ratio controller, particularly after feed flow rate increases, thereby resulting in a more timely and significant steam temperature increase in the stripping section, as compared to the case caused by the reflux flow.

This problem renders it difficult to achieve stable regulatory control by using the Q_R/F and R/F controllers simultaneously in one

(b) 20% Feed Composition Disturbances; CS2

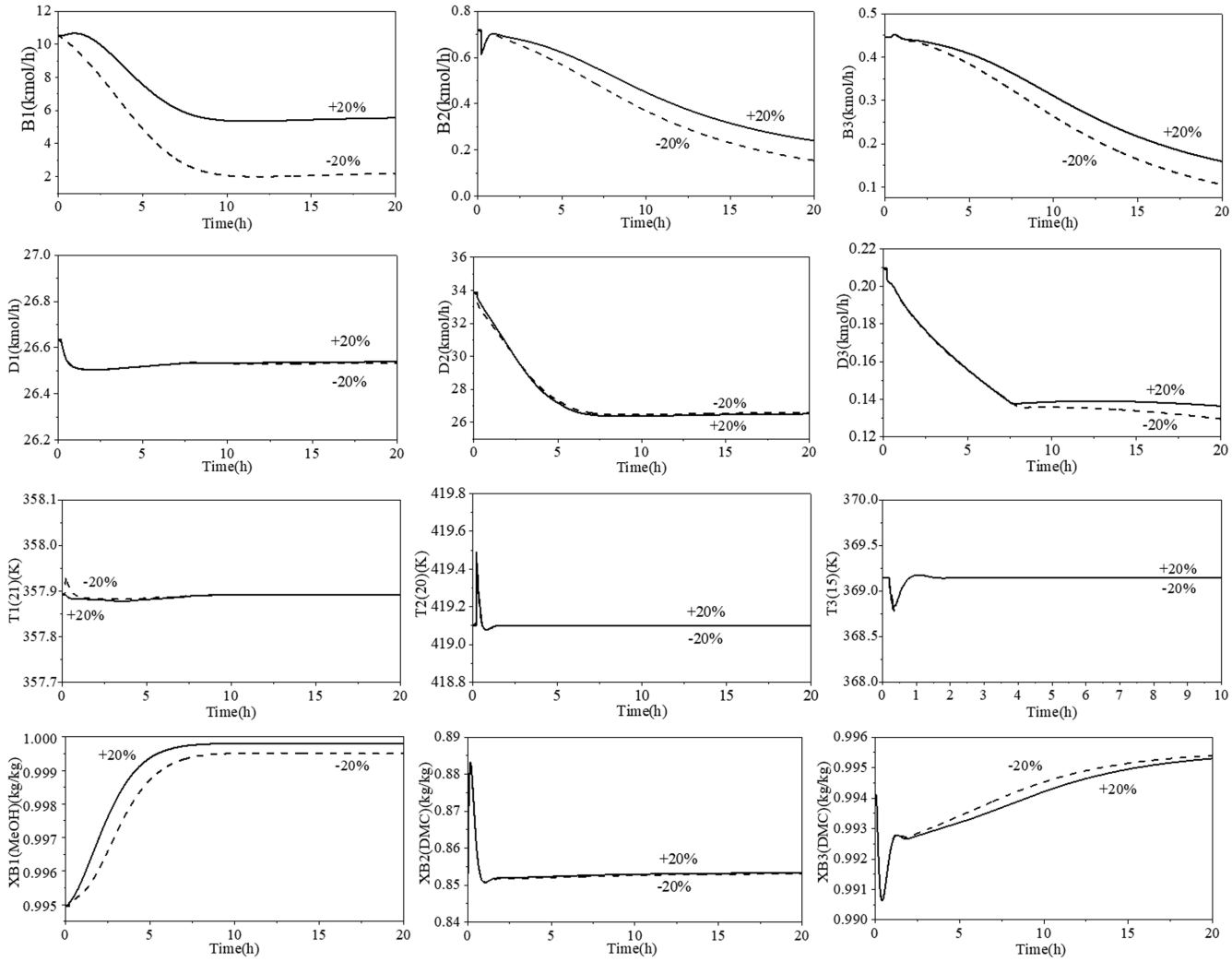

Fig. 9. Continued.

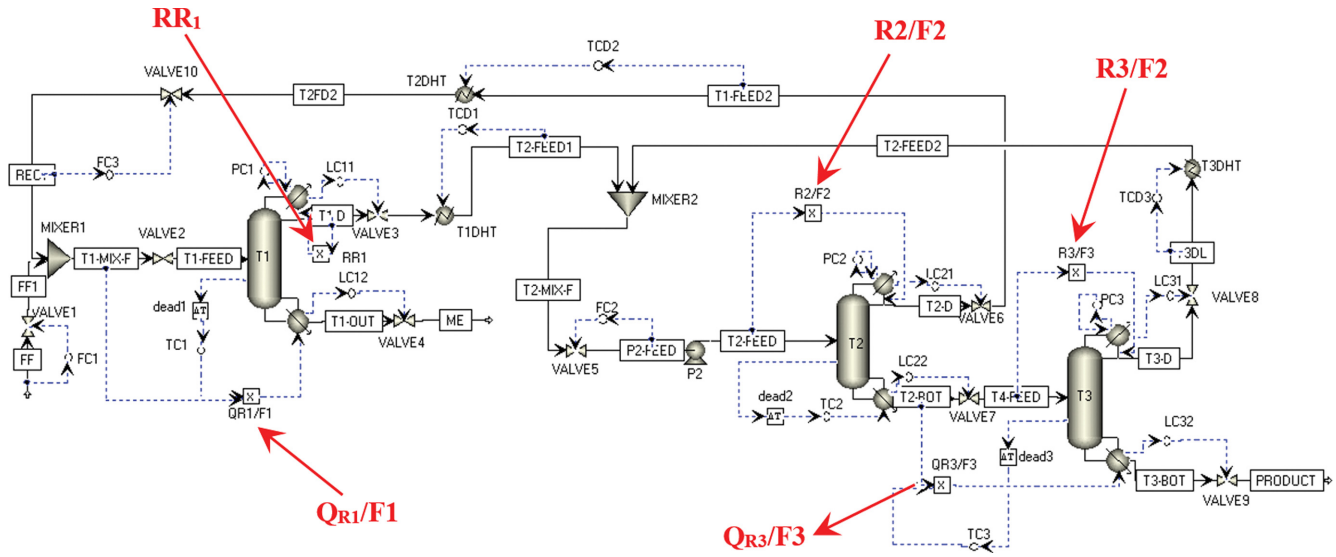

Fig. 10. Modified control structure CS3.

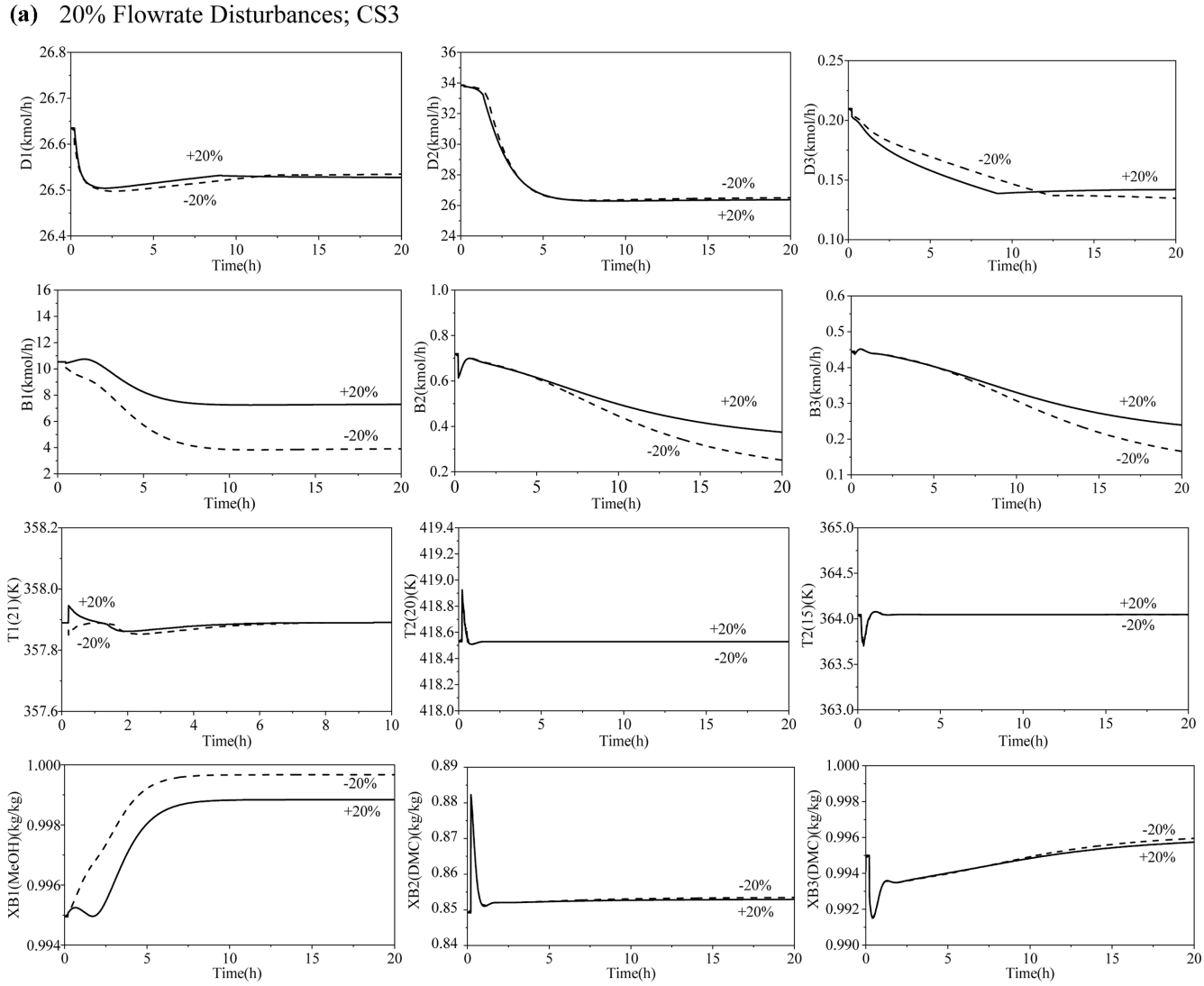

Fig. 11. CS3: (a) 20% changes in feed flowrate. (b) 20% changes in feed composition.

column.

4. Modified Control Structure CS3

A revised control scheme, where a feedforward ratio controller Q_R/F with a reflux-to-distillate ratio controller was used in T1, was implemented in the control structure CS3 (Fig. 10). Another important loop from the control perspective was administered, specifically where the flow controller FC3 controlled the flow rates of the recycled streams fed to column T1. The various loops differed from the basic control scheme CS1 in the following features:

1. The 21th tray temperature of the column T1 is adjusted by manipulating the reboiler heat input-to-feed ratio (Q_{R1}/F_1);
2. The reflux in column T2 is rationed to the feed (R2/F2);
3. The reflux in column T3 is rationed to the feed (R3/F3);
4. The 15th tray temperature of the column T3 is adjusted by manipulating the reboiler heat input-to-feed ratio (Q_{R3}/F_3);
5. The flow rates of the recycled streams fed to the column T1 are controlled using the flow (FC3).

Table 3 gives temperature transmitter ranges, controller output ranges and several tuning parameters of CS1, 2 and 3.

Fig. 11 shows how product concentration change in face of the same disturbances used previously. Fig. 11(a) presents the dynamic performance for a 20% step change in the flow controller (FC1) setpoint, where the setpoint was first increased and then decreased at a time t=0.2 h. The dashed lines define the 20% decrease. It was found in Fig. 11(a) that the three bottom products, namely, B1, B2, and B3, increased with the fresh feed flowrate. A good dynamic control system performance was found that the control scheme CS3 can maintain three bottoms product purity close to their desired level: 99.9 wt% MeOH in bottom product of T1, 85 wt% DMC in bottom product of T2 and 99.5 wt% DMC in bottom product of T3. Stable regulatory control was achieved.

Similar dynamic responses were obtained for the +20% feed DMC composition disturbance, where the solid lines define an increase of DMC concentration in the feed from 0.109 wt% to 0.131 wt%, and the dashed lines define a decrease of DMC concentration in the feed from 0.109 wt% to 0.087 wt%. These disturbances were handled well by the proposed control, which eliminated the X_{B1} purity problem observed in the basic control structure CS1

(b) 20% Feed Composition Disturbances; CS3

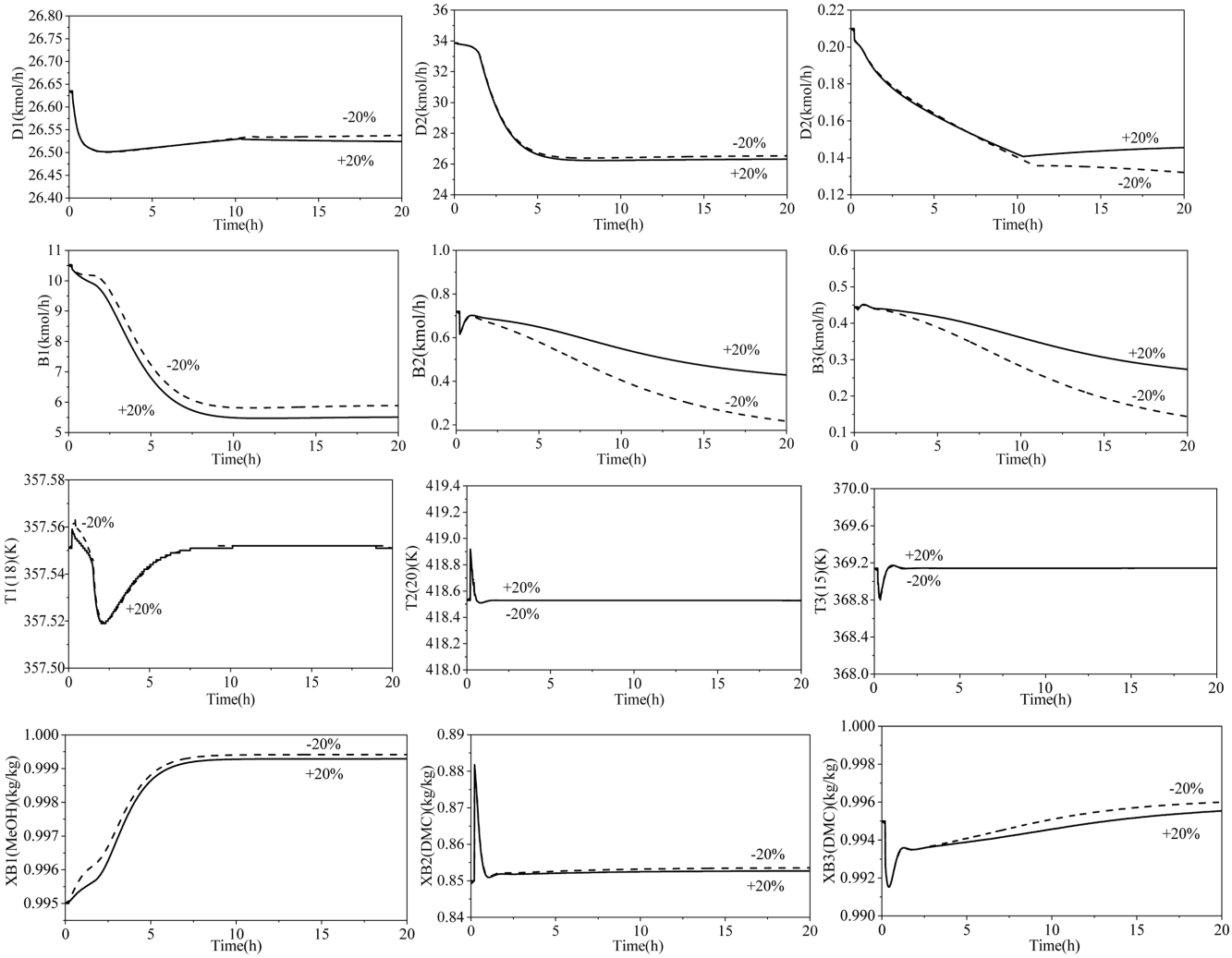

Fig. 11. Continued.

(Fig. 11(b)).

DISCUSSION

The main loop features of CS1, 2 and 3 are listed in Table 4.

Compared with CS1, the control strategy CS3 was significantly reliable in that the three bottom product purities are all close to their specified values Notably, it took about five hours for the three bottom product concentrations to stabilize at a new steady state value for fluctuations of feed flow rate. Compared to other two control schemes, the control strategy CS3 exhibited tighter control with smaller transient deviation and shorter setting time for fluctuations of feed flow rate. However, compared with CS1, the bottom purity X_{B1} and X_{B3} in both CS2 and CS3 significantly fluctuated with the feed composition disturbances; it took more time for bottom product X_{B3} to stabilize at a new steady state value.

Notice that the distillate product D, bottom product B, and the bottom purity X_B of the three columns significantly fluctuated with the feed flow disturbances, while the change trend of the distillate purity on top of the three columns was relatively slow. In particular, the bottom product B suddenly decreased, fluctuated, and finally stabilized after it ran for 10 h. It was noticed that the system rides through these disturbances fairly well except for the bottom purity X_{B1} (MeOH) of T1, and which dropped to almost 99.2 wt% after a 20% increase in the feed flowrate, while X_{B3} (DMC) tended to 1 regardless of the 20% increase and decrease in the disturbances of the feed flowrate.

In control scheme CS1, due to the implementation of the multiplier blocks RR and Q_{R1}/F1, the liquid flowrate (L_R) on the top tray and the upstream flowrate (Vs) on the bottom tray will be proportionally increased with the feed flowrate increases. As a result, more heavier component MeOH will be removed from the top of T1; this results in a drop in MeOH concentration X_{B1} (MeOH) from the bottom of T1. Similar results were obtained from step changes in the feed composition. Increasing feed DMC concentration results in an increase in X_{D1} (DMC) (See Fig. 7(b)). That is why X_{B1} (MeOH) deviated from its setpoint as +20% disturbances in feed flow rate and feed composition.

Table 3. Controller tuning parameters

Parameters	CS1	CS2	CS3
TC1			
Controlled variable	$T_{1,21}$	$T_{1,21}$	$T_{1,21}$
Manipulated variable	QR_1	QR_1/F_1	QR_1/F_1
Transmitter range (°C)	0-168.80	0-168.80	0-168.80
Controlled output range (GJ/h)	0-4.29	0-0.09	0-0.09
Ultimate gain	0.70	1.02	1.15
Ultimate period	3.6	4.8	3
K_C	0.17	0.17	0.17
τ_1 (min)	7.92	7.92	7.92
TC2			
Controlled variable	$T_{2,20}$	$T_{2,20}$	$T_{2,20}$
Manipulated variable	QR_2	QR_2	QR_2
Transmitter range (°C)	0-294.12	0-294.12	0-294.12
Controlled output range (GJ/h)	0-5.87	0-5.87	0-5.87
Ultimate gain	0.38	0.27	0.33
Ultimate period	2.4	4.8	3
K_C	0.12	0.12	0.12
τ_1 (min)	6.6	6.6	6.6
TC3			
Controlled variable	$T_{3,15}$	$T_{3,15}$	$T_{3,15}$
Manipulated variable	QR_3	QR_3/F_3	QR_3/F_3
Transmitter range (°C)	0-181.79	0-181.79	0-181.79
Controlled output range (GJ/h)	0-0.02	0-0.02	0-0.02
Ultimate gain	0.95	1.79	2.82
Ultimate period	6.6	9	6
K_C	0.82	0.82	0.82
τ_1 (min)	5.28	5.28	5.28

Table 4. The main loop features of CS1, 2 and 3

Parameters	T1	T2	T3
CS1			
Top			
Controlled variable			
Manipulated variable	RR_1	RR_2	RR_3
Bottom			
Controlled variable	$T_{1,21}$	$T_{2,20}$	$T_{3,15}$
Manipulated variable	QR_1	QR_2	QR_3
CS2			
Top			
Controlled variable			
Manipulated variable	R_1/F_1	R_2/F_2	R_3/F_3
Bottom			
Controlled variable	$T_{1,21}$	$T_{2,20}$	$T_{3,15}$
Manipulated variable	QR_1/F_1	QR_2	QR_3/F_3
CS3			
Top			
Controlled variable			
Manipulated variable	RR_1	R_2/F_2	R_3/F_3
Bottom			
Controlled variable	$T_{1,21}$	$T_{2,20}$	$T_{3,15}$
Manipulated variable	QR_1/F_1	QR_2	QR_3/F_3

In control scheme CS3, the application of the two multiplier blocks Q_{R1}/F_1 and RR1 in T1 results in an immediate change in reflux (L_{R1}) and reboiler heat input (Q_{R1}) as the feed flowrate increases: An increase in the feed flowrate produces an immediate increase in the vapor flowrate (V_{R1}) from the T1 bottom, the reflux flow (L_{R1}) immediately increases with using the ratio controller RR1. Further, the application of the ratio controller R2/F2 makes an immediate increase in the reflux (L_{R2}) and an decrease in distillate (D2), that is, the return flow recycled back to T1. Thus, the feed flowrate (T1-MIX-F) growth will be offset. And the application of the ratio controller R3/F3 makes an immediate decrease in distillate (D3), that is, the return flow recycled back to T2 decreases. In summary, the control scheme CS3 eliminates the X_{B1} purity problem. The purities of three bottom products are held closer to their desired values, and these results should be compared with those given in Fig. 7.

The analyses above provide a theoretical help to understand why X_{B1} (MeOH) is held quite close to the product specification following a +20% feed flowrate and feed composition disturbances.

CONCLUSION

This study explored the economic design and effective control for the multi-unit separation process of the DMC/MeOH azeotrope. Steady-state simulation was carried out with commercial software Aspen Plus.

The optimized steady-state configuration with three columns and two recycle streams was presented, which are NT_1=34, NT_2=24, NT_3=12. Furthermore, the optimized design can save 15.28% total annual cost, though the total annual costs of T2 and T3 are higher than the original one.

Three control strategies were explored and tested by large disturbances, and dynamic simulations were carried out with commercial software, Aspen Dynamics. The first scheme, CS1, with reflux-to-feed ratio controller applied in each column and reboiler heat input-to-feed ratio controller in T1, handles the feed disturbances fairly well except for the bottom purity X_{B1} (MeOH) of T1. Further, an improved structure CS2, with reflux-to-feed ratio in each column and reboiler heat input-to-feed ratio in T1 and T3, which makes the bottom level of T1 fell to zero after run initiation. To reduce the steady-state offsets in feed changes, the scheme CS3 was successively put forward; three distillation columns can be effectively controlled using fixed reboiler heat input-to-feed ratios and fixed reflux ratio in T1, fixed reboiler heat input-to-feed ratios and fixed reflux-to-feed ratio in both T2 and T3, which maintains the product purity closely in each column.

The control scheme CS3 can maintain three bottoms product purity close to their desired level, which eliminates the XB_1 purity problem; however, the bottom flowrates B2, B3 gradually decrease to a low flowrate. This is indeed a limitation for CS3. An improved control scheme which can maintain three bottoms product purity as well as keep productivity and operational stability deserves further investigation.

ACKNOWLEDGEMENTS

This work was supported by Science Foundation of North University of China (2015): Design and Control of Pressure-Swing separation of Azeotrope in Process Equipment (No: 110246) and Foundation of Shanxi Province Key Laboratory of Higee-Oriented Chemical Engineering (No: CZL2020-06).

NOTATION

TAC : total annual cost [$/year]
N_T : total number of column trays
N_F : feed tray location of a column
D : distillate flowrate [kmol/s]
B : bottom flowrate [kmol/s]
RR : reflux ratio
R/F ratio : reflux to feed ratio
V_S/F : ratio of the vapor flowrate from the bottom of the column to the feed flowrate
L_R : reflux flow
V_R : vapor flowrate on the second stage in distillation column
L_S : liquid flowrate on the second stage of the column
V_S : vapor flowrate from the bottom of the column
D : column diameter [m]
D : distillate flowrate [kmol/s]
B : bottom flowrate [kmol/s]
Q_R : reboiler heat input [GJ/h]
Q_C : condenser heat removal [GJ/h]
A_C : reboiler heat transfer area [m^2]
A_R : condenser heat transfer area [m^2]
Shell : shell capital cost [10^6 $]
HX : heat exchanger cost [10^6 $]
Energy : energy cost per year [10^6 $/y]
PI : proportional and integral
K_c : gain
τ_1 : integral time
CSn : n^{th} control strategy
Q_R/F : ratio of reboiler heat input to feed
X_{B1} : MeOH purity at the bottoms of the concentration column [kg/kg]
X_{B2} : MeOH purity at the bottoms of the pressured column [kg/kg]
X_{B3} : DMC purity at the bottoms of the refinery column [kg/kg]
X_{D1} : MeOH purity in the distillate stream of the concentration column [kg/kg]

REFERENCES

1. A. O. Esan, A. D. Adeyemi and S. Ganesan, *J. Clean. Prod.*, **257**, 120561 (2020).
2. P. Kumar, V. C. Srivastava, U. L. Stangar, B. Music, I. M. Mishra and Y. Meng, *Catal. Rev. Sci. Eng.*, **63**, 363 (2021).
3. S. R. Labafzadeh, K. J. Helminen, I. Kilpelainen and A. W. T. King, *ChemSusChem*, **8**, 77 (2015).
4. M. Selva, A. Perosa, D. Rodriguez-Padron and R. Luque, *ACS Sust. Chem. Eng.*, **7**, 6471 (2019).
5. K. T. Tan, K. T. Lee and A. R. Mohamed, *Fuel*, **89**, 3833 (2010).
6. T. Weidlich, *Chem. Listy.*, **109**, 594 (2015).
7. J. Sun, B. Yang and H. Lin, *Chem. Eng. Technol.*, **27**, 435 (2004).
8. C. S. Li, X. P. Zhang, S. J. Zhang and Q. Q. Xu, *Chin. J. Process Eng.*, 453 (2003).
9. S. J. Wang, C. C. Yu and H. P. Huang, *Comput. Chem. Eng.*, **34**, 361 (2010).
10. J. L. Zhang, F. Wang, W. C. Peng, F. K. Xiao, W. Wei and Y. H. Sun, *Petrochem. Eng.*, **39**, 646 (2010).
11. K. Y. Hsu, Y. C. Hsiao and I. L. Chien, *Ind. Eng. Chem. Res.*, **49**, 735 (2010).
12. H. M. Wei, F. Wang, J. L. Zhang, B. Liao, N. Zhao, F. K. Xiao, W. Wei and Y. H. Sun, *Ind. Eng. Chem. Res.*, **52**, 11463 (2013).
13. W. B. Zhao, F. Wang, W. C. Peng, N. Zhao, J. P. Li, F. K. Xiao, W. Wei and Y. H. Sun, *Ind. Eng. Chem. Res.*, **47**, 5913 (2008).
14. D. F. Wang, X. L. Zhang, W. Wei and Y. H. Sun, *Chem. Eng. Technol.*, **35**, 2183 (2012).
15. H. M. Wei, University of Chinese Academy of Sciences dissertation (2013).
16. X. B. Ma, X. G. Liu, Z. H. Li and G. H. Xu, *Fluid Phase Equilib.*, **221**, 51 (2004).
17. W. L. Luyben, *Distillation design and control using AspenTM simulation*, John Wiley & Sons: Inc: New York (2006).
18. J. D. Perkins, *J. Chem. Technol. Biot.*, **46**, 249 (1989).
19. R. Turton, R. C. B., W. B. Whiting and J. A. Shaeiwitz, *Org. Proc. Res: Dev.*, **3**, 494 (1999).
20. Y. J. Lin, D. Wong, S. H. D., S. S. Jang and J. J. Ou, *AIChE J.*, **58**, 2697 (2012).
21. W. L. Luyben, *AIChE J.*, **52**, 2290 (2006).
22. W. L. Luyben, *AIChE J.*, **52**, 623 (2006).
20. J. D. Ward, C. C. Yu and M. F. Doherty, *AIChE J.*, **53**, 2885 (2007).
23. V. G. Grassi, Practical Distillation Control (1992).
24. W. L. Luyben, *Ind. Eng. Chem. Res.*, **39**, 973 (2000).
25. W. L. Luyben, *AIChE J.*, **57**, 655 (2011).